

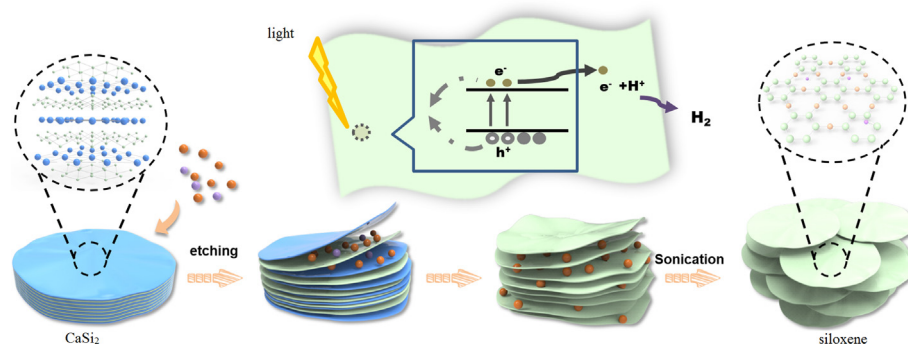
One-step controllable synthesis of amino-modification siloxene for enhanced solar water-splitting



Liping Zhou, Yang Wang, Xinling Xu, Weisheng Lei, Jingyun Huang^{*}, Lingxiang Chen, Liping Zhu, Zhizhen Ye^{*}

School of Materials Science and Engineering, State Key Laboratory of Silicon Materials, Key Laboratory for Biomedical Engineering of Ministry of Education, Zhejiang University, Hangzhou 310027, China

GRAPHICAL ABSTRACT



ARTICLE INFO

Article history:

Received 2 April 2020

Revised 11 June 2020

Accepted 14 June 2020

Available online 16 June 2020

Keywords:

Two-dimensional nanosheets

Siloxene

Amino modification

Water-splitting

ABSTRACT

Novel two-dimensional silicon-based material siloxene has been synthesized handily by a one-step method, which utilizes the characteristics of the topological exfoliation to simplify the process of synthesis and modification. It is worth mentioning that for the first time amino-modified derivative has been investigated. Amino modification can promote the oxidation of siloxene, enlarge the bandgap and extend the carrier lifetime of siloxene. The application of siloxene before and after modification in water-splitting has been investigated. In addition, the superiority of the resultant two-dimensional materials was concisely elaborated, which revealed that owing to more effective photogenerated carriers' separation in amino modification siloxene, hydrogen production could be greatly promoted.

© 2020 Elsevier Inc. All rights reserved.

1. Introduction

Since the successful preparation of graphene by Geim and Novoselov in 2004 [1], it has ushered in a new era for two-dimensional material research [2]. In recent years, there have been countless reports about the application of graphene, and nearly all

kinds of novel properties of graphene have been explored. However, the study of its two-dimensional (2D) silicon counterpart is not as intense as that of graphene. Two-dimensional silicon materials also have several unique properties [2–5], and because of the wide application of silicon-based materials in the field of integrated circuits, solar cells and light-emitting, 2D (with nanometer-thickness) silicon materials also have great significance in long-term research. Over the past decades, some progress in 2D silicon-based materials has already been made, including the the-

^{*} Corresponding authors.

E-mail addresses: huangjy@zju.edu.cn (J. Huang), yezz@zju.edu.cn (Z. Ye).

oretical calculations and preliminary experimental research. In 1994, Takeda and Shiraishi [6] studied the graphite-like structure of silicon and germanium through the first principle and discussed the planarity of their two-dimensional atomic layers. In 2012, a large area of silicene has been synthesized on Ag (111) surface by epitaxial growth, which verified the theoretical prediction of silicene [7]. Deficiently, previous studies were relatively unsystematic, and there was no distinction between subdivision types (ultrathin silicon crystal nanosheets, silicene, siloxene), which led to the confusion of the concept of 2D silicon-based materials.

Besides, there are still many restrictions and obstacles in the preparation of 2D silicon materials, such as limited preparation methods and poor controllability [8]. MBE method [9] is a mature choice for the preparation of silicene, through which, pure and layer-controlled silicene could grow epitaxially on specific substrates such as Ag(111) [10], SiC(0001) [11] and Ir(111) [12]. Nevertheless, the operation of MBE is so complex and cost-intensive, which hinders large-scale research. Besides, the performance of silicene prepared by MBE is greatly affected by the substrate materials. The template-assisted magnesium thermal reduction method is commonly used for the preparation of ultrathin silicon nanosheets, and the as-synthesized samples possess better crystallinity and controllable sheet size [13–18]. The deficiency of this method is that it can only prepare silicon crystal sheets, and graphene-like silicene/siloxene structure cannot be prepared via this method. Topo-chemical exfoliation is another common method for the preparation of 2D material [19–21]. Utilizing the natural planar net-connection structure of Si atomic layer in CaSi_2 , the Ca^{2+} in CaSi_2 could be specifically etched by a proper oxidant such as concentrated hydrochloric acid and I_2 to obtain silicene/siloxene. By adjusting the parameters [22,23] (solvent system, reaction temperature, oxidant selection) of the reaction system, different oxidation degree of siloxene or even pure silicene can be obtained, and the aim of exploring the most appropriate reaction conditions. At the current stage, pure silicene is so sensitive to the ambient environment [24] which greatly limits the practical application. Hence, we decide to start with the research of siloxene, which possesses a similar structure and more chemically inert surface.

Siloxene, a 2D silicon oxide with unique low-buckled structure, has attracted increasing attention in recent years due to its novel properties [25,26]. There are two different structures of siloxene [27]: Wohler siloxene and Kautsky siloxene. Wohler siloxene can be regarded as the encapsulated silicene: with the upper surface encapsulated by hydrogen atoms and the lower surface encapsulated by hydroxyl. However, Wohler siloxene is as highly unstable as silicene. Kautsky siloxene can be regarded as the derivate of the Wohler siloxane that the oxygen atoms in the hydroxyl of Wohler siloxene enter into the Si atomic surface for doping, and the Si atoms form independent six-fold rings, which are connected by oxygen atoms and extend to a plane [25,28]. Kautsky siloxene has the lowest free energy, so it keeps a stable structure that facilitates the study of its various properties. However, due to the randomness of doping oxygen atoms, Kautsky siloxene has an amorphous phase.

As commonly known, crystalline silicon is a kind of common indirect band gap semiconductor ($E_g = 1.1$ eV). Its first direct band gap is about 3.4 eV. The calculated results show that the ordered and environment-sensitive Wohler siloxene has a direct bandgap of 1.5–2.7 eV [29], while the inert and amorphous Kautsky siloxene has a larger indirect bandgap. The electronic structure of Kautsky siloxene makes it worth studying in the field of photocatalysis. Compared with crystalline FCC-structure silicon, π -junction system of siloxene increases the bandgap and facilitates the separation of photo-generated charges [30,31]. As a typical 2D material, siloxene has a large specific surface area, consequently generating

more surface-active sites as well as improving mass transfer capability. Abundant hanging groups on the surface of siloxene play a vital role in the process of catalysis [32]. In a word, siloxene has such a bright future in the application of catalysis, nevertheless, the relevant research is sparse, let alone further modification.

In our research work, the energy band structure of siloxene has been effectively optimized and the visible-light harvesting efficiency has been dramatically improved via controlling the thickness and providing some surface functionalization to siloxene. In addition, compared with common photocatalysts, the preparation cost of siloxene is considerably lower because of the abundance of silicon in the Earth's crust, and the topological chemical method used in this paper is facile and cheap in raw materials, which cater for actual production demand in future work. In addition, the components of siloxene are environmentally friendly and without biological hazards, which makes it a green candidate.

2. Materials and methods

2.1. Synthesis procedure

At air atmosphere, 1.705 g $\text{CuCl}_2 \cdot 5\text{H}_2\text{O}$ (Sinopharm Chemical Reagent Co., Ltd) was dissolved into 100 mL anhydrous alcohol, then 0.97 g CaSi_2 powder (Ourchem Chemical Reagent Co., Ltd) was added into the solution slowly (mole ratio = 1:1). After 3 h of reaction, the mixture was centrifuged and the sedimentation was carefully collected. The as-received precipitation was dispersed into absolute ethanol with supersonic vibration, then the red suspension was well collected. Repeat the ultrasound process several times and the as-synthesized siloxene nanosheet powder, after washing by dilute HCl, was obtained by vacuum drying. To synthesis amino-functionalized siloxene nanosheets, 0.053 g NH_4Cl (10% of the quantity of $\text{CuCl}_2 \cdot 5\text{H}_2\text{O}$) was added as nitrogen source and other steps remained invariant.

2.2. Characterization

The obtained powder was identified by powder X-Ray diffraction using Shimadzu XRD-6000 with a $\text{Cu K}\alpha$ radiation ($\lambda = 1.5406$ Å) operating at 40 kV and 150 mA. The visual surface topography was studied by SEM (Hitachi S-4800) and STEM (FEI Tecnai G2F20S-TWIN). Thickness measurement were performed on AFM (Veeco MultiMode). Structure and chemical composition were tested via FTIR (Nicolet5700) and X-ray photoelectron spectroscopy (Thermo Scientific K-Alpha +)

2.3. Optical characterization

For PL measurements (FLS920), pure siloxene nanosheets and amino-functionalized siloxene nanosheets were dispersed into absolute ethanol and the solution was put into a quartz cuvette with a path length of 1 cm, and excited by the pulse laser ($\lambda = 405$ nm). The measured data were corrected for the ethanol cuvette background.

3. Results

CaSi_2 powder is bedded-rock shaped, as shown in Fig. S1, Ca^{2+} ion layers and Si^- atom network is closing piled by electrovalent bond. Fig. 1 showed the preparation strategy of siloxene. Cl^- could weaken the interaction between Ca^{2+} and Si atom web, while Cu^{2+} will be inserted into the compact structure meanwhile reducing to Cu particle. The intermediate product appeared as an interesting morphology that layer siloxenes piled up loosely with Cu particles inserted among them. Ultrasound treatment and rinsing made the

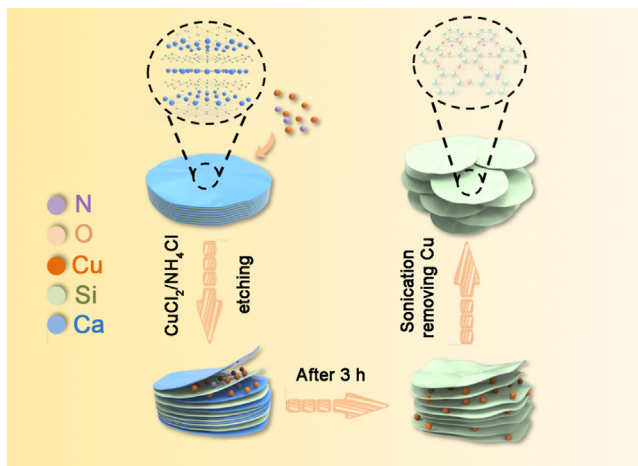


Fig. 1. Schematic illustration of the strategy for the preparation of pure siloxene/amino modification siloxene.

intermediate product dispersing to ultrathin nanosheets. It is a common idea to utilize the unique structure of CaSi_2 to obtain silicene/siloxene, but our concern is how to obtain the uniform and large-area nanosheets while maintaining ultrathin characteristic. The crux is the oxidant and the solvent system, that is, the oxidation ability of oxide and the polarity of solvent need to be adaptive. Most previous researchers used concentrated HCl aqueous solution to obtain siloxene. However, CaSi_2 can react with water to produce explosive gas SiH_4 and tiny amounts of white precipitate containing Ca, so that products obtained in this way is of poor quality. After trying different chlorides (FeCl_3 , CuCl_2 , ZnCl_2 , SnCl_2) and carrying out the reaction in different solvent systems, it is concluded that nanosheets with large lateral size and best uniformity can be obtained in ethanol with CuCl_2 as oxidant. In this paper, emphasis was put on the siloxene, which can effectively be separated from

Cu particles by ultrasonic-centrifugation owing to the large density difference between intermediates.

The as-prepared siloxene nanosheet was an amorphous sample, proved by XRD (Fig. 2a), which was consistent with Krishnamoorthy's result. As displayed in Fig. S4, the pre-ultrasound-treatment siloxenes, which were not fully distributed, were stacked in layers and looked like steps. As is shown in Fig. 2b–c, the free-standing siloxene nanosheets were several atom layers, with lateral size larger than 500 nm and the morphology is similar to its IV group 2-dimension analogue, graphene. The height of the siloxene was around 3.2 nm measured by AFM (Fig. 2d), in accordance with the STEM result.

As commonly known, bare silicon surface is unstable and therefore hydroxyl groups and hydrogen atoms are easily trapped by Si plane. Fig. 3a is the result of Fourier Transform Infrared Spectrum, which shows: Both two samples had 1637 cm^{-1} , $1050\text{--}1150\text{ cm}^{-1}$ and 460 cm^{-1} characteristic peaks, corresponding to O–H bending modes, Si–O–Si stretching modes and Si–O–Si bending vibrations, respectively. The broad peak of the pure sample near 3400 cm^{-1} was caused by O–H stretching modes and the peak near 2100 cm^{-1} was assigned to Si–H stretching. There was a peak near 875 cm^{-1} for the pure sample but not for the amino sample which was corresponding to Si–H₂ scissors and similarly at 648 cm^{-1} is Si–H bending. The peak near 520 cm^{-1} was Si–Si in Si plane. From FTIR, the following detailed structure conclusions were obtained: 1. The amino groups were successfully modified on the surface of siloxene; 2. Compared with the modified SO, the pure SO surface has more –H hanging bonds; 3. After the amino modification, more oxygen atoms were doped into the Si plane.

X-ray photoelectron spectroscopy was performed to investigate the components of the as-prepared samples. It was observed that the Si in pure-SO (siloxene nanosheets) existed mainly in the form of +4 valences (Fig. 3b), and others in the form of lower valence. Meanwhile, after amino-modification, the Si atoms in amino-SO were totally oxidized (Fig. 3c). Both XPS and EDS (Fig. S7) demonstrated the successful modification of nitrogen-containing

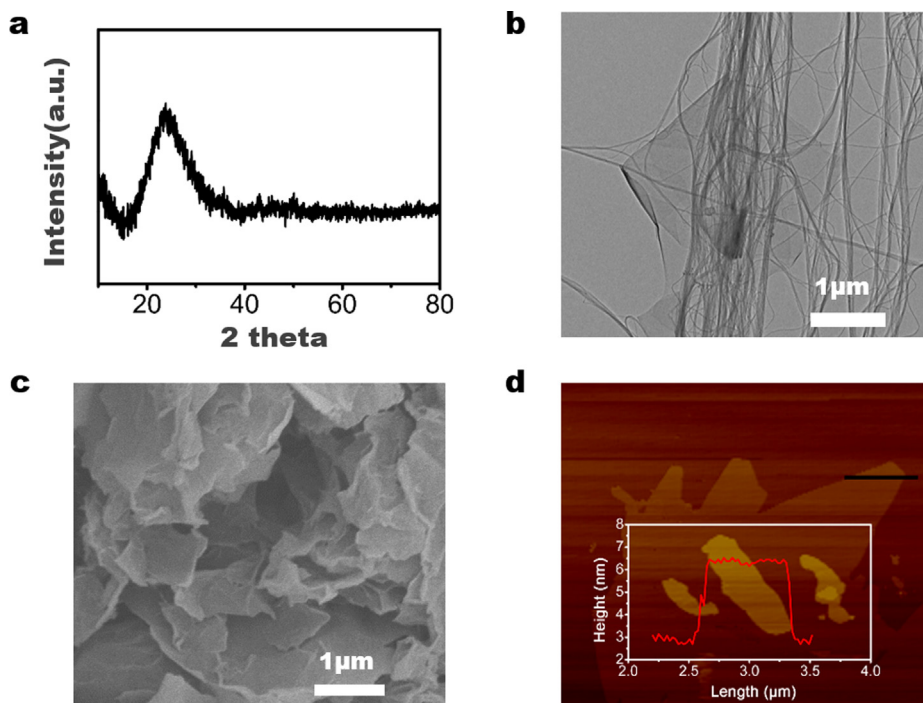


Fig. 2. (a) XRD image of pure-SO (b) TEM image of the as-prepared siloxene on CNT micro grid (c) TEM image of the as-prepared siloxene, (d) AFM of the as-prepared siloxene nanosheets, with thickness about 3.2 nm.

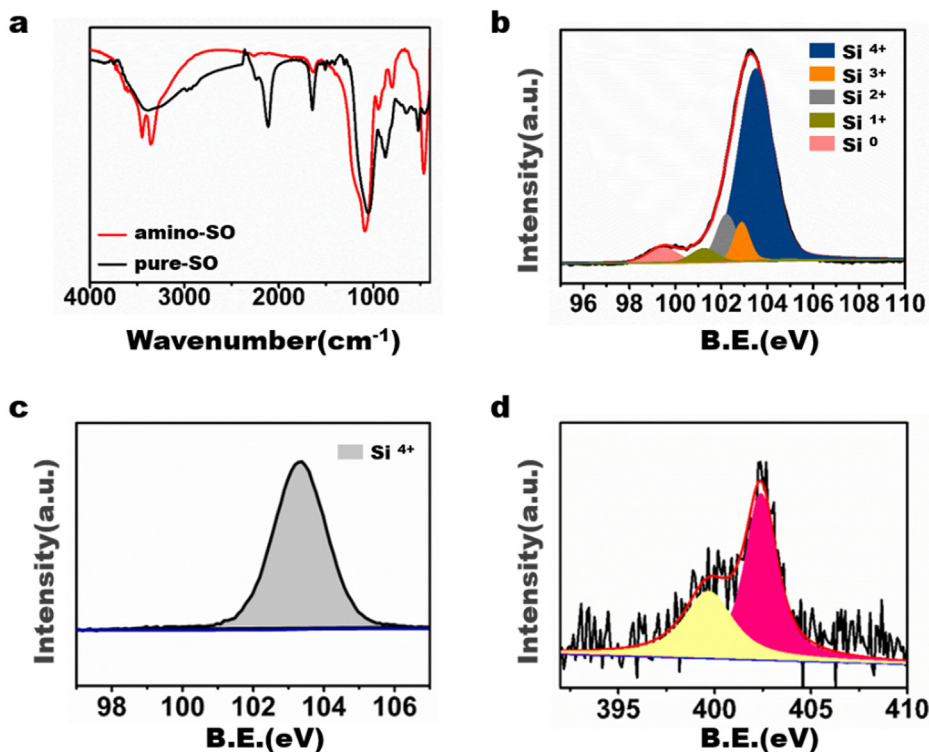


Fig. 3. (a) FTIR of pure-SO and amino-SO, (b) XPS Si 2p spectra of pure-SO (c) XPS Si 2p spectra of amino-SO, (d) XPS N spectra of amino-SO.

groups in the sample synthesized by $\text{NH}_4\text{Cl}/\text{CuCl}_2$ co-reaction and Fig. 3d showed that N atoms existed in the form of amino groups, connecting with Si atoms. In the process of oxidation and stripping of CaSi_2 by chlorides, Ca^{2+} ions were dissolved into the solution and at the same time, abundant active sites were formed on the surface of the exposed Si plane. A large amount of heat was released from the reaction, so the amino modification could be completed in the

reaction process without the aid of external pressure or heat source.

For further exploration of the electrical properties of pure siloxene and the effect of amino modification on its band structure, UV-visible diffuse reflectance test (DRS) and photoluminescence spectroscopy were performed. Fig. 4a implied that the bandgap of the pure-SO was about 1.92 eV, close to the absorption range of red

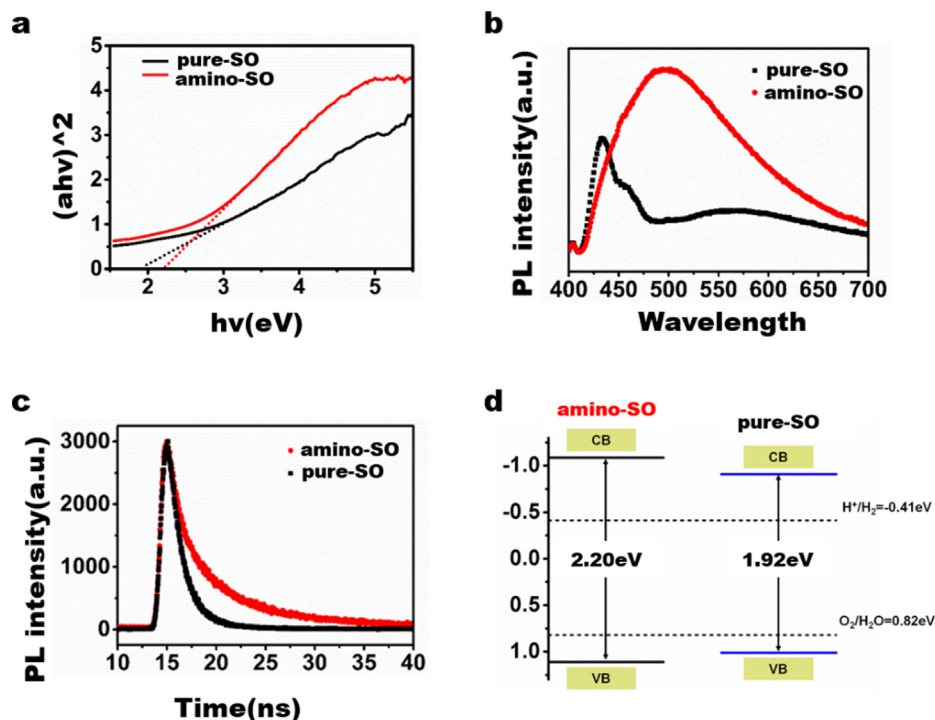


Fig. 4. (a) UV-vis diffuse reflectance spectrum of SO (b) PL excitation spectra of pure-SO/amino-SO (excited at 405 nm) (c) Time-resolved PL spectrum monitored at 430 nm under 405 nm excitation at 298 K for pure-SO and at 520 nm for amino-SO (d) Band structure of siloxene.

light (620–760 nm), while amino-modification could slightly enlarge the bandgap, and the bandgap of amino-SO was 2.20 eV. Compared with the common semiconductor photocatalysts, TiO_2 (3.2 eV) [33], $\text{g-C}_3\text{N}_4$ (2.7 eV) [34], the bandgap of SO was greatly reduced, which meant that the SO could make full use of visible light and consequently greatly improve the efficiency of sunlight harvesting and utilization. The PL spectra of two SO samples were measured to further understand the energy band structure. The results showed that the positions of the strongest peaks of the two samples are quite different. The emission peak of pure-SO is near 430 nm, while amino modification results in emission peak broadening and redshift, and the strongest emission peak is near 500 nm, close to the bandwidth measured by DRS.

A probe into carrier separation was performed by time-resolved photoluminescence spectrum (Fig. 4b), which clearly indicated that the carrier lifetime of amino-SO ($\tau = 3.08$ ns) was about 1 time longer than pure-SO ($\tau = 1.53$ ns). Longer carrier lifetime represented more efficient hole-electron separation because it meant more time for carriers to migrate to the surface for redox reactions to catalyze hydrogen production before recombination. To elaborate on the valence band position and flat band potential, the Mott-Schottky plots were employed. As is shown in Fig. S8, both samples equipped a positive slope, indicating a typical *n*-type semiconductor. After several Mott-Schottky tests at different frequencies, it showed that the flat band potential of pure-SO was -0.91 eV (vs. Ag/AgCl), and that of amino-SO was -1.09 eV (vs. Ag/AgCl). Compared with the reduction potential of H^+/H_2 (-0.4 eV), there were enough reasons to believe that amino modification promoted the reduction of hydrogen. Combined with the above tests, the band structure of this novel 2D silicon-based material could be figured out, as is shown in Fig. 4d. The energy band structures of the two samples met the requirements of the HER. More than this, the bandgap was narrow enough so that it was sensitive to visible light, which was more exceptional than the

common metal-free photocatalysts. After amino modification, the efficiency of carrier separation was improved, mainly due to the inhibition of hole-electron pair recombination, and this was also supported by the photocurrent test results (Fig. S9).

The photocatalytic activity of as-obtained siloxene nanosheets was measured by evaluating the hydrogen yield with or without co-catalyst. Taking the narrow bandgap of siloxene into account, we didn't only use Xe-lamp as the simulated solar light source, but also used ordinary mixed white light as the visible light source to measure the hydrogen yield. Methanol was added as a sacrificial agent to consume the holes produced in the reaction. As shown in Fig. 5a, when a simulated solar light source was employed to provide solar energy, the hydrogen production of pure-SO was relatively minor ($37.0 \mu\text{mol/g}$) without Pt co-catalyst, and the hydrogen production of amino-modified sample was estimated to be $121.4 \mu\text{mol/g}$, which was 478% higher than that of pure-SO. After Pt was added as co-catalyst, the hydrogen production of pure-SO increased to $76.7 \mu\text{mol/g}$, which was more than three times that of pure-SO without co-catalyst. Although the hydrogen production of amino-SO also increased partially, the promotion effect of co-catalyst was not as obvious as that in pure-SO, and the hydrogen production reached $175.0 \mu\text{mol/g}$, 44% higher than that of amino-SO without co-catalyst. And compared with pure-SO under the same conditions, the hydrogen production after amino modification nearly doubled.

Similarly, under a visible light source, the hydrogen production of pure SO reached $12.0 \mu\text{mol/g}$ without Pt as co-catalyst, and the hydrogen production of amino-modified sample was $28.7 \mu\text{mol/g}$. After adding Pt as co-catalyst, the hydrogen production of pure-SO increased significantly to $39.6 \mu\text{mol/g}$, more than three times of that without co-catalyst. That of amino-SO reached $53.6 \mu\text{mol/g}$, and compared with pure-SO under the same conditions, the hydrogen production after amino modification increased by 37%.

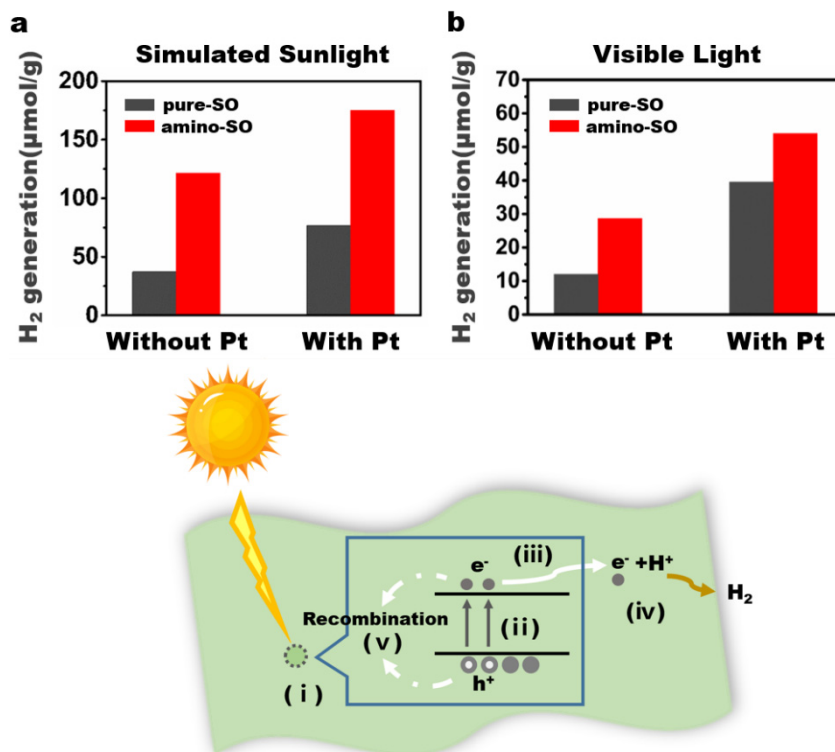


Fig. 5. (a) Hydrogen generation amount of pure-SO/amino-SO under the radiation of Xe lamp to simulate sunlight. (b) Hydrogen generation amount of pure-SO/amino-SO under the visible light. The figure below is the Schematic illustration of the pre-water splitting process in siloxene.

It could be seen that under visible light conditions, although the hydrogen production after amino modification had a certain increase, the promotion degree was far less than that of the simulated solar light source, because the bandgap of pure-SO was smaller than that of amino-SO, so it could make full use of visible light. Under the condition of visible light, the heterojunction formed by Pt could promote hydrogen production more effectively, and under the simulated sunlight, the amino modification was more effective.

To ascertain the reason for the significant improvement of photocatalytic performance by amino modification, the process of photocatalytic reaction can be carefully broken down into the following processes: (i) When the light hits the surface of the material, photocatalyst absorbs part of the optical energy which is larger than its bandgap; (ii) The electrons in the ground state absorb energy and then transition, and generates free electron-hole pair; (iii) Part of the effectively separated electron migrate to the catalyst surface (iv) At the active site of the reaction, H^+ ionized in water is reduced to H_2 by these free electrons; (v) Another part of photo-generated electron-hole pair fails to carry out effective catalytic reaction, that is, recombination in vivo or on the surface.

Because the bandgap of pure-SO is narrower than that of amino-SO, theoretically pure-SO has more advantages for step (i): it can use more light of a wider range. Next, we would analyze step (ii): The absorption spectra of pure-SO and amino-SO show that the as-obtained siloxene is an indirect bandgap semiconductor, however, from the result of PL spectrum, the peak intensity of amino-SO is higher than that of pure-SO, at the same time the carrier lifetime of amino-SO is longer than that of pure-SO, and the peak wavelength of pure-SO with smaller bandgap is smaller than that of amino-SO. Considering the above points, we can reasonably surmise that amino-SO is more likely to generate carriers than a pure sample. In other words, amino modification changes the momentum gap between the minimum conduction band (the bottom of the conduction band) and the maximum full band in K space, that is to say, amino modification makes the energy band of siloxene more "direct", which is helpful for the generation of electron-hole pairs. The step (iii) and step (v) are a pair of competing processes. In the photocatalytic reaction, we expect to promote the step (iii) and inhibit the step (v). According to the measured carrier lifetime, amino group modification can prolong the carrier lifetime and allow more time for electrons to migrate to the surface active sites, this is because $-NH_2$ is more electronegative than $-OH$ and $-H$ dangling on the surface of siloxene and thus facilitating the separation of photo-excited electrons from holes. As for step (iv), the electrons which successfully migrated to the surface-active site reacted with H^+ , and the characteristics of 2D materials shortened the migration path and abated the in-bulk recombination. Therefore, amino group modification can promote the efficiency of hydrogen production by promoting the separation of electrons and holes. This inference is also verified by the results of adding Pt as co-catalyst. Pt particles can form heterojunction with siloxene and promote the separation of carriers, so the hydrogen production of pure-SO increases 300% after adding Pt, while the promotion effect of cocatalyst on amino-SO is evidently weaker.

4. Conclusions

Herein, we have successfully synthesized ultrathin 2D siloxene nanosheets via a simple and scalable topological exfoliation approach, and the amino surface modification was carried out for the first time. We have systematically demonstrated the effect of amino modification on its energy band structure. The resultant amino-modified siloxene nanosheets can effectively separate carriers, simultaneously they have the advantages of narrowing the

bandgap of siloxene and superiority structure of 2D material. Amino modification further boosts the carrier separation which greatly improved hydrogen production efficiency over 478% compared with pure siloxene under the simulated sunlight.

CRedit authorship contribution statement

Liping Zhou: Methodology, Investigation, Writing - original draft. **Yang Wang:** Validation. **Xinling Xu:** Data curation. **Weisheng Lei:** Data curation. **Jingyun Huang:** Conceptualization, Writing - review & editing, Supervision. **Lingxiang Chen:** Resources. **Liping Zhu:** Resources. **Zhizhen Ye:** Resources, Supervision.

Declaration of Competing Interest

The authors declare that they have no known competing financial interests or personal relationships that could have appeared to influence the work reported in this paper.

Acknowledgment

This work was financially supported by Zhejiang Provincial Public Technology Research (LGG18E020001) and the National Natural Science Foundation of China (Grant91833301).

Appendix A. Supplementary data

Supplementary data to this article can be found online at <https://doi.org/10.1016/j.jcis.2020.06.066>.

References

- [1] K.S. Novoselov, A.K. Geim, S.V. Morozov, D. Jiang, Y. Zhang, S.V. Dubonos, I.V. Grigorieva, A.A. Firsov, Electric Field Effect in Atomically Thin Carbon Films, *Science* 306 (5696) (2004) 666.
- [2] W. Tao, N. Kong, X. Ji, Y. Zhang, A. Sharma, J. Ouyang, B. Qi, J. Wang, N. Xie, C. Kang, H. Zhang, O.C. Farokhzad, J.S. Kim, Emerging two-dimensional monoelemental materials (Xenes) for biomedical applications, *Chem. Soc. Rev.* 48 (11) (2019) 2891–2912.
- [3] N.D. Drummond, V. Zolyomi, V.I. Fal'ko, Electrically tunable band gap in silicene, *Phys. Rev. B* 85 (7) (2012) 075423.
- [4] U. Kim, I. Kim, Y. Park, K.-Y. Lee, S.-Y. Yim, J.-G. Park, H.-G. Ahn, S.-H. Park, H.-J. Choi, Synthesis of Si Nanosheets by a Chemical Vapor Deposition Process and Their Blue Emissions, *ACS Nano* 5 (3) (2011) 2176–2181.
- [5] L.C. Loaiza, L. Monconduit, V. Seznec, Siloxene: A potential layered silicon intercalation anode for Na, Li and K ion batteries, *J. Power Sources* 417 (2019) 99–107.
- [6] K. Takeda, K. Shiraishi, Theoretical possibility of stage corrugation in Si and Ge analogs of graphite, *Phys. Rev. B* 50 (20) (1994) 14916–14922.
- [7] P. Vogt, P. De Padova, C. Quaresima, J. Avila, E. Frantzeskakis, M.C. Asensio, A. Resta, B. Ealet, G. Le Lay, Silicene: Compelling Experimental Evidence for Graphenelike Two-Dimensional Silicon, *Phys. Rev. Lett.* 108 (15) (2012) 155501.
- [8] A. Kara, H. Enriquez, A.P. Seitsonen, L.C. Lew Yan Voon, S. Vizzini, B. Aufray, H. Oughaddou, A review on silicene – New candidate for electronics, *Surface Science Reports*, 67(1) (2012) 1–18.
- [9] N. Gao, J.C. Li, Q. Jiang, Bandgap opening in silicene: Effect of substrates, *Chem. Phys. Lett.* 592 (2014) 222–226.
- [10] C.-L. Lin, R. Arafune, K. Kawahara, N. Tsukahara, E. Minamitani, Y. Kim, N. Takagi, M. Kawai, Structure of Silicene Grown on Ag(111), *Appl. Phys Express* 5 (4) (2012) 045802.
- [11] P. Li, X. Li, W. Zhao, H. Chen, M.-X. Chen, Z.-X. Guo, J. Feng, X.-G. Gong, A.H. MacDonald, Topological Dirac States beyond π -Orbitals for Silicene on SiC (0001) Surface, *Nano Lett.* 17 (10) (2017) 6195–6202.
- [12] L. Meng, Y. Wang, L. Zhang, S. Du, R. Wu, L. Li, Y. Zhang, G. Li, H. Zhou, W.A. Hofer, H.-J. Gao, Buckled Silicene Formation on Ir(111), *NANO Lett.* 13 (2) (2013) 685–690.
- [13] K. Adpakpang, S.B. Patil, S.M. Oh, J.-H. Kang, M. Lacroix, S.-J. Hwang, Effective Chemical Route to 2D Nanostructured Silicon Electrode Material: Phase Transition from Exfoliated Clay Nanosheet to Porous Si Nanoplate, *Electrochimica Acta* 204 (2016) 60–68.
- [14] S. Chen, Z. Chen, X. Xu, C. Cao, M. Xia, Y. Luo, Scalable 2D Mesoporous Silicon Nanosheets for High-Performance Lithium-Ion Battery Anode, *Small* 14 (12) (2018).

- [15] W.-S. Kim, Y. Hwa, J.-H. Shin, M. Yang, H.-J. Sohn, S.-H. Hong, Scalable synthesis of silicon nanosheets from sand as an anode for Li-ion batteries, *Nanoscale* 6 (8) (2014) 4297–4302.
- [16] Z. Lu, D. Sim, W. Zhou, W. Shi, H.H. Hng, Q. Yan, Synthesis of Ultrathin Silicon Nanosheets by Using Graphene Oxide as Template, *Chem. Mater.* 23 (24) (2011) 5293–5295.
- [17] J. Ryu, D. Hong, S. Choi, S. Park, Synthesis of Ultrathin Si Nanosheets from Natural Clays for Lithium-Ion Battery Anodes, *ACS Nano* 10 (2) (2016) 2843–2851.
- [18] P.P. Wang, Y.X. Zhang, X.Y. Fan, J.X. Zhong, K. Huang, Synthesis of Si nanosheets by using Sodium Chloride as template for high-performance lithium-ion battery anode material, *J. Power Sources* 379 (2018) 20–25.
- [19] T. Morishita, K. Nishio, M. Mikami, Formation of single- and double-layer silicon in slit pores, *Phys. Rev. B* 77 (2008) 81401.
- [20] H. Nakano, T. Mitsuoka, M. Harada, K. Horibuchi, H. Nozaki, N. Takahashi, T. Nonaka, Y. Seno, H. Nakamura, Soft Synthesis of Single-Crystal Silicon Monolayer Sheets, *Angewandte Chemie International Edition* 45 (38) (2006) 6303–6306.
- [21] J. Lang, B. Ding, S. Zhang, H. Su, B. Ge, L. Qi, H. Gao, X. Li, Q. Li, H. Wu, Scalable Synthesis of 2D Si Nanosheets, *Adv. Mater.* 29 (31) (2017).
- [22] K. Xu, L. Ben, H. Li, X. Huang, Silicon-based nanosheets synthesized by a topochemical reaction for use as anodes for lithium ion batteries, *Nano Res.* 8 (8) (2015) 2654–2662.
- [23] S.-Y. Oh, H. Imagawa, H. Itahara, Si-based nanocomposites derived from layered CaSi₂: influence of synthesis conditions on the composition and anode performance in Li ion batteries, *J. Mater. Chem. A* 2 (31) (2014) 12501–12506.
- [24] L. Tao, E. Cinquanta, D. Chiappe, C. Grazianetti, M. Fanciulli, M. Dubey, A. Molle, D. Akinwande, Silicene field-effect transistors operating at room temperature, *Nat. Nanotechnol.* 10 (3) (2015) 227–231.
- [25] P. Deák, M. Rosenbauer, M. Stutzmann, J. Weber, M.S. Brandt, Siloxene: Chemical quantum confinement due to oxygen in a silicon matrix, *Phys. Rev. Lett.* 69 (17) (1992) 2531–2534.
- [26] K. Krishnamoorthy, P. Pazhamalai, S.-J. Kim, Two-dimensional siloxene nanosheets: novel high-performance supercapacitor electrode materials, *Energy Environ. Sci.* 11 (6) (2018) 1595–1602.
- [27] H.D. Fuchs, M. Stutzmann, M.S. Brandt, M. Rosenbauer, J. Weber, A. Breitschwerdt, P. Deák, M. Cardona, Porous silicon and siloxene: Vibrational and structural properties, *Phys. Rev. B* 48 (11) (1993) 8172–8189.
- [28] Y. Wang, L. Zhou, J. Huang, X. Wang, X. Xu, J. Lu, Y. Tian, Z. Ye, H. Tang, S.-T. Lee, Y. Lu, Highly Stable Lithium–Sulfur Batteries Promised by Siloxene: An Effective Cathode Material to Regulate the Adsorption and Conversion of Polysulfides, *Adv. Funct. Mater.* 30 (12) (2020) 1910331.
- [29] M. Stutzmann, M.S. Brandt, M. Rosenbauer, H.D. Fuchs, S. Finkbeiner, J. Weber, P. Deak, Luminescence and optical properties of siloxene, *J. Lumin.* 57 (1) (1993) 321–330.
- [30] S. Li, H. Wang, D. Li, X. Zhang, Y. Wang, J. Xie, J. Wang, Y. Tian, W. Ni, Y. Xie, Siloxene nanosheets: a metal-free semiconductor for water splitting, *J. Mater. Chem. A* 4 (41) (2016) 15841–15844.
- [31] H. Itahara, H. Nakano, Synthesis and optical properties of two-dimensional nanosilicon compounds, *Japanese Journal of Applied Physics*, 56(5S1) (2017) 05DA02.
- [32] R. Ramachandran, X. Leng, C. Zhao, Z.-X. Xu, F. Wang, 2D siloxene sheets: A novel electrochemical sensor for selective dopamine detection, *Appl. Mater. Today* 18 (2020) 100477.
- [33] H. Xiong, L. Wu, Y. Liu, T. Gao, K. Li, Y. Long, R. Zhang, L. Zhang, Z.-A. Qiao, Q. Huo, X. Ge, S. Song, H. Zhang, Controllable Synthesis of Mesoporous TiO₂ Polymorphs with Tunable Crystal Structure for Enhanced Photocatalytic H₂ Production, *Adv. Energy Mater.* 9 (31) (2019) 1901634.
- [34] G. Liao, Y. Gong, L. Zhang, H. Gao, G.-J. Yang, B. Fang, Semiconductor polymeric graphitic carbon nitride photocatalysts: the “holy grail” for the photocatalytic hydrogen evolution reaction under visible light, *Energy Environ. Sci.* 12 (7) (2019) 2080–2147.